Risk publications

Risk

RISK MANAGEMENT • DERIVATIVES • REGULATION

Risk.net August 2020

Cutting edge
Volatility modelling

A new arbitrage-free parametric volatility surface

A new arbitrage-free parametric volatility surface

Alexandre Antonov, Michael Spector and Michael Konikov describe a new parametric volatility surface that is arbitrage free, is extremely rich and flexible, and has closed-form expressions for both European option values and local volatilities. The volatility surface is based on previous work by Carr and Pelts, for which the present authors provide a simple derivation and a concrete implementation

Parametric volatility surfaces are used in finance and financial modelling for many purposes, such as:

- vanilla option pricing, risk, hedging and market making;
- data cleansing, information reduction and producing derived data;
- arbitrage detection and prevention, trade signals;
- scenario generation and volatility surface dynamics; and
- as an input for stochastic models, ie, local volatility (LV) and local stochastic volatility (LSV) models.

A particularly important use of such surfaces is in Dupire's formulation of the LV model, where the parameterisation is employed to obtain derivatives of the implied volatility (or option price) that appear in Dupire's formula. The local volatility itself usually is not available analytically, but implied volatility (or option price) usually is. It is very important for the volatility surface not only to be free of any sort of arbitrage but also to be sufficiently smooth if we want to produce a sensible local volatility function using Dupire's formula. More generally, some desirable properties of a volatility surface are:

- absence of static arbitrage, or, equivalently, positivity of call spreads, butterfly spreads and calendar spreads (see, for example, Cousot 2004);
- parsimonious formulation, ie, the ability to describe the continuum of option prices with just a few parameters;
- flexibility, ie, the ability to fit as rich an options data set as needed (eg, the Standard & Poor's 500 (SPX));
- smoothness, which is an important feature to facilitate the use of Dupire's formula (see Dupire 1994);
- fast option valuation, preferably in closed form; and
- fast local volatility valuation, preferably in closed form.

It is usually very hard to guarantee the total absence of arbitrage working directly in the implied volatility space, since arbitrage conditions are difficult to translate into volatility terms. If we parameterise in the price space, however, we can ensure our surface is free of arbitrage, but then it is hard to achieve a plausible shape for its implied volatility.

One of the first parametric volatility surfaces that guaranteed the absence of arbitrage under some conditions was the stochastic volatility inspired (SVI) volatility surface introduced in Gatheral (2004) and Gatheral & Jacquier (2012, 2014). This has many desirable properties (although not all of those listed above) and is still very popular in the industry. Its shortcomings include a lack of flexibility to fit rich options data when arbitrage conditions are enforced as well as time-direction interpolation in price terms; strike interpolation at input maturities is, however, done in volatility terms. The latter may lead to some unintuitive shapes for the interpolated volatilities and may introduce arbitrage in the strike dimension.

The methodology first described in Carr & Pelts (2015) is somewhat unique in that it allows both a guarantee of no arbitrage and a reasonable shape of the implied volatility surface at the same time. Moreover, we show that both implied and local volatilities are known essentially in closed form. The only drawback of this surface is its restricted flexibility, similar to the SVI construction. The obvious reason for this is that the two-dimensional volatility surface is parameterised with two one-dimensional functions.

The contribution of the present article is to provide a simplified explanation of how the Carr-Pelts (CP) surface can be implemented in practice as well as a generalisation allowing for a much more flexible (possibly arbitrarily flexible) surface able to fit very rich sets of options data. We also show how to incorporate discrete dividends into the construction of our volatility surface. Going forward, we refer to our new volatility surface (first introduced in Antonov *et al* (2019)) as the ensemble Carr-Pelts (ECP) surface.

The CP surface

In this section, we provide some intuition behind the CP construction. Take a stochastic variable X with cumulative distribution $\Psi(k) = \mathbb{E}[1_{X<k}]$ such that $\mathbb{E}[\mathrm{e}^X]$ exists and equals 1. Define a function $F(\cdot)$ mapping the distribution into its measure change version (an interval $[0, 1]$ to $[0, 1]$) as follows:

$$F(\mathbb{E}[1_{X<k}]) := \mathbb{E}[\mathrm{e}^X 1_{X<k}]$$

or, explicitly:

$$F(u) := \mathbb{E}[\mathrm{e}^X 1_{X<\Psi^{-1}(u)}]$$

implying:

$$F'(u) = \mathrm{e}^{\Psi^{-1}(u)} \quad \text{and} \quad F''(u) = \frac{\mathrm{e}^{\Psi^{-1}(u)}}{\Psi'(\Psi^{-1}(u))}$$

Note that knowing $F(u)$ allows us to find the distribution $\Psi(k)$ and that $F(1) = 1$ is equivalent to $\mathbb{E}[\mathrm{e}^X] = 1$. Also, both $F'(u)$ and $F''(u)$ are positive, which means $F(u)$ is increasing and convex.

Now, consider an exponential martingale process X_t with $\mathbb{E}[\mathrm{e}^{X_t}] = 1$ and cumulative distribution $\Psi(t, k)$. We extend the previous considerations from the stochastic variable to the process by adding the time argument:

$$F(t, u) := \mathbb{E}[\mathrm{e}^{X_t} 1_{X_t<\Psi_u^{-1}(t,u)}]$$

where the inverse of u is taken for a fixed t, and, like before, we have:

$$\partial_u F(t, u) = \mathrm{e}^{\Psi_u^{-1}(t,u)} \tag{1}$$

$$\partial_u^2 F(t, u) = \frac{\mathrm{e}^{\Psi_u^{-1}(t,u)}}{\partial_u \Psi(\Psi_u^{-1}(t, u))}$$

Again, the function $F(t, u)$ is increasing and convex in u. One can prove that $F(t, u)$ is decreasing in time. Indeed, a 'European put option' value can

be expressed as:

$$\mathbb{E}[(\mathrm{e}^k - \mathrm{e}^{X_t})^+] = \mathrm{e}^k \Psi(t,k) - F(t, \Psi(t,k)) \tag{2}$$

Since X_t is an exponential martingale, the option value should be increasing in time, giving us:

$$0 \leqslant \mathrm{e}^k \partial_t \Psi(t,k) - \partial_u F(t, \Psi(t,k)) \partial_t \Psi(t,k) - \partial_t F(t, \Psi(t,k)) = -\partial_t F(t, \Psi(t,k))$$

where we used the following identity:

$$\partial_u F(t, \Psi(t,k)) = \mathrm{e}^{\Psi^{-1}(t, \Psi(t,k))} = \mathrm{e}^k$$

For example, for a Gaussian process $X_t = W_t - \frac{1}{2}t$, the function F reads:

$$F_{\mathrm{G}}(t,u) = N(N^{-1}(u) - \sqrt{t}) \tag{3}$$

Now, we would like to find a function $F(t,u)$ that satisfies the properties above and has a richer structure than the Gaussian one $F_{\mathrm{G}}(t,u)$. To 'enrich' it in u, Carr and Pelts proposed replacing the Gaussian cumulative distribution function (cdf) $N(\cdot)$ with some cdf $\Omega(\cdot)$, so:

$$F(t,u) = \Omega(\Omega^{-1}(u) - \sqrt{t}) \tag{4}$$

Define a function $h(\cdot)$ underlying the derivative of $\Omega(\cdot)$:

$$\Omega(x) = \int_{-\infty}^{x} \mathrm{d}x' \, \mathrm{e}^{-h(x')} \tag{5}$$

Then, for any convex function $h(\cdot)$ with derivative limits:

$$\lim_{z \to \pm\infty} h'(z) = \pm\infty$$

the function $F(t,u)$ is increasing and convex in u and decreasing in time. The proof is based on the derivative of (4):

$$\partial_u F(t,u) = \frac{P_\Omega(\Omega^{-1}(u) - \sqrt{t})}{P_\Omega(\Omega^{-1}(u))} \tag{6}$$

where $P_\Omega(\cdot)$ is a density of the distribution $\Omega(\cdot)$:

$$P_\Omega(z) = \Omega'(x) = \mathrm{e}^{-h(z)} \tag{7}$$

So, the Gaussian structure corresponding to a parabola:

$$h(x) = \frac{x^2 + \log(2\pi)}{2}$$

was enriched to an arbitrary convex function.[1] Note that in our numerical experiments we chose it to be piecewise quadratic polynomial.

To determine the distribution function $\Psi(t,u)$ of the process X_t corresponding to (4), we use (1), (6) and (7) to obtain the inverse (in the space variable) cdf:

$$\Psi_u^{-1}(t,u) = h(\Omega^{-1}(u)) - h(\Omega^{-1}(u) - \sqrt{t}) \tag{8}$$

This formula gives an explicit link between a stochastic variable Q corresponding to the cdf Ω, $\mathbb{E}[1_{Q<x}] = \Omega(x)$, and the variable X_t. Namely, if we evaluate the expression (8) for a uniformly distributed stochastic variable U and take into account that:

$$Q \sim \Omega^{-1}(U), \qquad X_t \sim \Psi_u^{-1}(t,U)$$

we obtain:

$$\mathrm{e}^{X_t} \sim \frac{P_\Omega(Q - \sqrt{t})}{P_\Omega(Q)} \tag{9}$$

The marginal probability form (9) permits us to illustrate certain properties of e^{X_t}, eg, its unit average:

$$\begin{aligned}\mathbb{E}[\mathrm{e}^{X_t}] &= \int \mathrm{d}q \, P_\Omega(q) \frac{P_\Omega(q - \sqrt{t})}{P_\Omega(q)} \\ &= \int \mathrm{d}q \, P_\Omega(q - \sqrt{t}) \\ &= \int \mathrm{d}(q - \sqrt{t}) \, P_\Omega(q - \sqrt{t}) \\ &= 1\end{aligned}$$

and a growing second moment. Indeed, for a convex function $h(\cdot)$, define:

$$H(q,\tau) = h(q) - 2h(q+\tau) + h(q+2\tau)$$

on $\tau \in [0, +\infty)$. Then, since h is convex, h' is increasing and:

$$\partial_\tau H(q,\tau) = 2(h'(q+2\tau) - h'(q+\tau)) > 0$$

which implies that H is increasing in τ. Now:

$$\begin{aligned}\mathbb{E}[\mathrm{e}^{2X_t}] &= \int \mathrm{d}q \, P_\Omega(q) \frac{P_\Omega^2(q - \sqrt{t})}{P_\Omega^2(q)} \\ &= \int \mathrm{d}q \, \frac{P_\Omega^2(q - \sqrt{t})}{P_\Omega(q)} \\ &= \int \mathrm{d}q \, \mathrm{e}^{-2h(q+\sqrt{t}) + h(q+2\sqrt{t})}\end{aligned}$$

which proves that the second moment is increasing as well.

CP formula for European put. For any fixed pair of t and k, using a numerical solver for $z(t,k) = \Omega^{-1}(\Psi(t,k))$ in (8):

$$h(z(t,k)) - h(z(t,k) - \sqrt{t}) = k \tag{10}$$

we easily obtain the desired cdf:

$$\mathbb{E}[1_{X_t < k}] = \Psi(t,k) = \Omega(z(t,k))$$

The measure-changed cdf $\mathbb{E}[\mathrm{e}^{X_t} 1_{X_t<k}]$ also has a simple form:

$$\begin{aligned}\mathbb{E}[\mathrm{e}^{X_t} 1_{X_t<k}] &= F(t, \Psi(t,k)) \\ &= \Omega(\Omega^{-1}(\Psi(t,k)) - \sqrt{t}) \\ &= \Omega(z(t,k) - \sqrt{t})\end{aligned}$$

such that the put option (2) reads:

$$\mathbb{E}[(\mathrm{e}^k - \mathrm{e}^{X_t})^+] = \mathrm{e}^k \Omega(z(t,k)) - \Omega(z(t,k) - \sqrt{t})$$

Finally, by a positive increasing time-change $t \to \tau(t)$, we obtain the CP formula:

$$\mathcal{P}(t,K) = \mathbb{E}[(K - \mathrm{e}^{X_t})^+] = K\Omega(\hat{z}(t,K)) - \Omega(\hat{z}(t,K) - \sqrt{\tau(t)}) \tag{11}$$

[1] *One can also prove that the formulation (4) remains valid for unimodal distributions $\Omega(\cdot)$ (see Lucic 2020).*

where $\hat{z}(t, K) = z(\tau(t), \log K)$. Explicit formulas for the non-unit forward and discount factor as well as its call option version can be found in Antonov *et al* (2019).

Algorithmically, we do the following. Having fixed the parameterisation functions $\tau(\cdot)$ and $h(\cdot)$, for any given t and K, we solve (10) for $\hat{z} = \hat{z}(t, K)$:

$$h(\hat{z}) - h(\hat{z} - \sqrt{\tau(t)}) = \log K \tag{12}$$

Then, the arbitrage-free price of the put option can be obtained using (11). Note that (12) always has a unique solution since $h(z)$ is convex (see Antonov *et al* (2019) for details).

In our implementation, we introduced a Black-Scholes-inspired, volatility-like piecewise constant function $\sigma(t)$ to define:

$$\tau(t) = \int_0^t \sigma^2(s)\,\mathrm{d}s$$

and a piecewise quadratic $C^1(\mathbb{R})$ function $h(z)$, so that as long as the main coefficients of each quadratic are positive, we are guaranteed that $h(z)$ is convex with:

$$\lim_{z\to\pm\infty} h'(z) = \pm\infty$$

LV formula. Let us obtain an analytic expression for the local volatility:

$$\mathrm{d}S_t = S_t \sigma_{\mathrm{LV}}(t, S_t)\,\mathrm{d}W_t$$

which matches the put option of CP (11):

$$\mathbb{E}[(K - S_t)^+] = \mathcal{P}(t, K)$$

This makes the parameterisation useful for an arbitrage-free parametric implied volatility surface and constitutes a first step in calibrating an LV model and possibly even an LSV model using Gyöngy's lemma (for fast calibration). From Dupire's formula:

$$\sigma^2_{\mathrm{LV}}(t, K) = \frac{2\,\partial_t \mathcal{P}(t, K)}{K^2 \partial^2_K \mathcal{P}(t, K)} \tag{13}$$

we can compute the local volatility (see more details in Antonov *et al* (2019)):

$$\sigma^2_{\mathrm{LV}}(t, K) = \frac{\sigma^2(t)(h'(\hat{z}) - h'(\hat{z} - \sqrt{\tau(t)}))}{\sqrt{\tau(t)}} \tag{14}$$

where $\sigma^2(t) := (\tau(t))'$. As expected, we can see that for the Black-Scholes case with $h'(z) = z$, the local volatility becomes the Black-Scholes volatility. We can also see that for the surface to be arbitrage free, it is necessary and sufficient that τ be a positive, non-decreasing function and that h be a convex function.

Small time analysis. For small times, we can explicitly express the function h using the local volatility σ_{LV}. The formula (12) can be inverted for small times, since it expands as:

$$h'(\hat{z}) = x + O(\sqrt{\tau(t)}) \tag{15}$$

for $x = \log K/\sqrt{\tau(t)}$, such that:

$$\hat{z} = h'^{-1}(x)$$

1 An example of a half-day Carr-Pelts surface local volatility

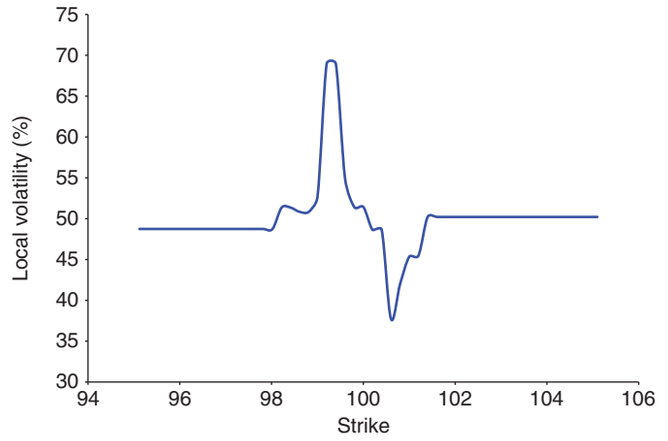

Similarly, from the local volatility expression (14) in the small time limit, we have:

$$\frac{\sigma^2_{\mathrm{LV}}(t, K)}{\sigma^2(t)} = h''(\hat{z}) + O(\sqrt{\tau(t)})$$

For a fixed t, by defining the volatilities ratio:

$$v(x) \equiv \frac{\sigma^2_{\mathrm{LV}}(t, \mathrm{e}^x\sqrt{\tau(t)})}{\sigma^2(t)} \simeq h''(h'^{-1}(x))$$

and by taking into account that:

$$h''(h'^{-1}(x)) = \frac{1}{(h'^{-1})'(x)}$$

we get:

$$V(x) \equiv \int_0^x \frac{\mathrm{d}x'}{v(x')} = h'^{-1}(x) \tag{16}$$

or, finally:

$$\int_0^y \mathrm{d}y'\, V^{-1}(y') = h(y) \tag{17}$$

So, if the local volatility is piecewise constant in the space variable, $V(x)$ (the integral of $1/v(x)$) is decreasing piecewise linear, as is its inverse $V^{-1}(y)$. Thus, $h(y)$ is piecewise quadratic. Conversely, a piecewise-quadratic $h(x)$ produces a piecewise-constant local volatility. We give an example of a half-day local volatility curve of a CP surface, which has a slightly smoothed piecewise-constant form, in figure 1.

ECP volatility surface

We note that although the CP surface is fairly flexible, it is trying to fit a surface with two curves, each roughly corresponding to each dimension of the surface (z does not correspond to the K-direction exactly, since solving for z involves T). Drawing inspiration from the tensor product basis, we can make the surface more flexible by taking a mixture of regular CP surfaces with some positive weights summing up to one. This results in the following

formula for option value:

$$\mathcal{P}(t,K) = \mathbb{E}[(K - \mathrm{e}^{X_t})^+]$$
$$= \sum_j w_j \left[K\Omega_j(\hat{z}_j(t,K)) - \Omega_j\left(\hat{z}_j(t,K) - \sqrt{\tau_j(t)}\right)\right] \quad (18)$$

$$\Omega_j(z) = \int \mathrm{e}^{-h_j(z)}\,\mathrm{d}z \quad (19)$$

$$\log K = h_j(\hat{z}_j(t,K)) - h_j\left(\hat{z}_j(t,K) - \sqrt{\tau_j(t)}\right) \quad (20)$$

and the following formula for local volatility:

$$\sigma^2_{\mathrm{LV}}(t,K) = \frac{\sum_j w_j \mathrm{e}^{-h_j(\hat{z}_j - \sqrt{\tau_j(t)})} \dfrac{\sigma_j^2(t)}{\sqrt{\tau_j(t)}}}{\sum_j w_j \dfrac{\mathrm{e}^{-h_j(\hat{z}_j - \sqrt{\tau_j(t)})}}{h_j'(\hat{z}_j) - h_j'(\hat{z}_j - \sqrt{\tau_j(t)})}} \quad (21)$$

where $\sigma_j^2(t) := \tau_j'(t)$. It is easy to see that if each τ_j is a positive increasing function and each h_j is a convex function, both the numerator and the denominator of (21) are positive, which implies that there is no arbitrage in our volatility surface.

Cash dividends

To use our ECP surface on equity options data, we need to be able to handle cash dividends. In this case, we decompose the stock process S_t into a pure dividend part and a martingale part (see Buehler (2018) and his other related work for a justification) as:

$$S_t = \tilde{S}_t + \sum_{\tau_k > t} D_k P(t,\tau_k), \qquad \tilde{S}_0 = S_0 - \sum_{\tau_k > 0} D_k P(0,\tau_k) \quad (22)$$

Note that:

$$S_t - K = \tilde{S}_t + \sum_{\tau_k > t} D_k P(t,\tau_k) - K = \tilde{S}_t - \tilde{K}$$

where:

$$\tilde{K} = K - \sum_{\tau_k > t} D_k P(t,\tau_k), \qquad \tilde{S}_t = \exp\left(\int_0^t r_s\,\mathrm{d}s\right) X_t \quad (23)$$

for some positive local martingale X_t. This means we can use the methodology introduced in the two previous sections on X_t instead of S_t, as long as we adjust the spot and strike values.

Practical use of the ECP volatility surface

Besides the obvious use of our surface for pricing and risk-managing vanilla options, it can also be used as an input for stochastic models. One such model is Dupire's LV model, described by the stochastic differential equation (SDE):

$$\frac{\mathrm{d}S_t}{S_t} = (r_t - q_t)\,\mathrm{d}t + \sigma_{\mathrm{LV}}(t,S_t)\,\mathrm{d}W_t$$

By having the local volatility function in closed form, we can easily implement this model using either finite-difference or Monte Carlo methods. Another popular model that can use our surface as input is the LSV model (Lipton 2002; Madan *et al* 2007), which is governed by the following SDEs:

$$\frac{\mathrm{d}S_t}{S_t} = (r_t - q_t)\,\mathrm{d}t + \sigma_{\mathrm{LSV}}(t,S_t)\lambda(t)\sqrt{z_t}\,\mathrm{d}W_t^1$$

2 Volatility surface of input options

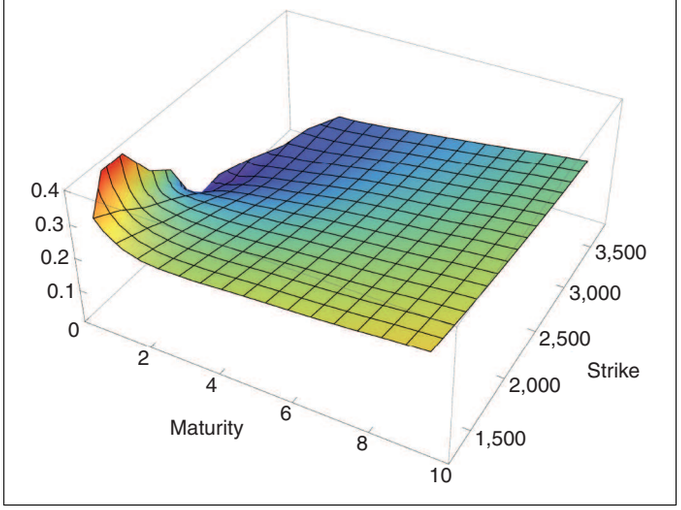

A. Summary of ECP results (errors are in spot basis points; timing is in seconds)

Test	Statistic: Average error	Max error	Timing
Calibration	4.58	17.45	3.11
Dupire	4.75	18.82	0.45
LSV	8.34	40.07	18.64

$$\mathrm{d}z_t = \kappa(t)(1 - z_t)\,\mathrm{d}t + \gamma(t)\sqrt{z_t}\,\mathrm{d}W_t^2$$
$$\mathrm{d}W_t^1\,\mathrm{d}W_t^2 = \rho(t)\,\mathrm{d}t$$

Gyöngy's theorem (Gyöngy 1986) can be employed to write:

$$\sigma^2_{\mathrm{LV}}(t,K) = \mathbb{E}[\sigma^2_{\mathrm{LSV}}(t,S_t)\lambda^2(t)z_t \mid S_t = K]$$

$$\sigma^2_{\mathrm{LSV}}(t,K) = \frac{\sigma^2_{\mathrm{LV}}(t,K)}{\lambda^2(t)\mathbb{E}[z_t \mid S_t = K]}$$
$$= \frac{\sigma^2_{\mathrm{LV}}(t,K)P_{S_t}(K)}{\lambda^2(t)\int_{\mathrm{D}(z_t)} z p_{S_t,z_t}(K,z)\,\mathrm{d}z}$$

and if we use forward induction as described in Andreasen & Huge (2011), we obtain probabilities recursively and can easily compute the expectations in the formula. Since our surface also gives us local volatility in closed form, we can obtain σ_{LSV} without any calibration.

Numerical results

We tested our ECP surface on the SPX options data for a number of dates in August 2017. Here, we present the results for August 1, but the results were similar for other dates. In our test, $S_0 = 2476.35$, $r = 1.1\%$–2.1%, $q = 2.82\%$, $T = 17\mathrm{D}$–$10\mathrm{Y}$ and $K = 1,238$–$3,715$. Figure 2 shows the input volatility surface. For ECP, we used three factors (an ensemble of three CPs) and 11 z-points, and we regularised the calibration by adding smoothness penalties with the tensions 10^{-2} for σ, 10^{-3} for γ and 10^{-2} for the resulting σ_{LV} to our least-squares objective function. The calibrated surface was used in Dupire's LV and LSV models with finite differences when pricing input options. The grid size for the finite-difference method was 300 time steps, 300

3 ECP calibration errors (spot basis points)

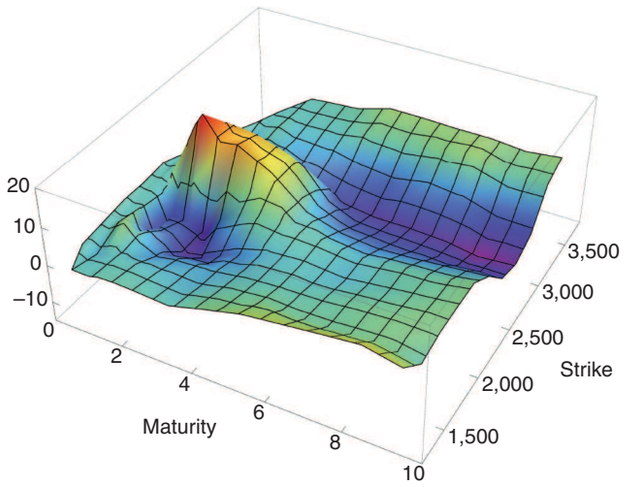

4 ECP calibration errors in volatility terms (volatility basis points)

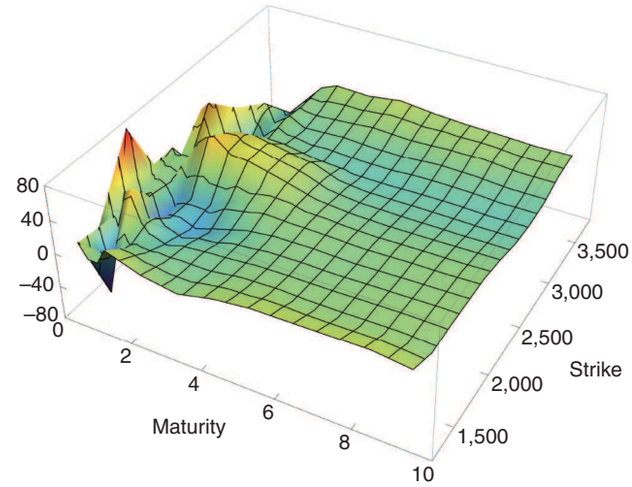

B. ECP calibration errors (spot basis points)

	K										
T	1,238	1,486	1,733	1,981	2,229	2,476	2,724	2,972	3,219	3,467	3,715
0.05	—	—	—	—	−0.02	0.64	—	—	—	—	—
0.12	—	—	−0.19	0.76	0.33	−0.01	—	—	—	—	—
0.22	—	−0.07	0.29	0.32	0.10	−0.01	−0.60	—	—	—	—
0.30	—	0.01	−0.01	−0.12	0.11	0.26	0.06	—	—	—	—
0.37	—	−0.21	−0.09	−0.22	0.15	0.63	1.68	—	—	—	—
0.62	0.15	−1.54	1.49	0.17	−0.94	0.83	5.14	−0.19	—	—	—
0.87	0.04	−0.79	3.11	−7.46	−7.05	8.79	1.94	1.02	—	—	—
1.14	0.06	−0.43	0.52	−4.19	−6.91	14.02	−0.33	−1.10	0.34	—	—
1.39	0.72	−0.14	−1.42	−4.82	−7.29	17.45	7.50	−2.82	−0.55	−0.32	—
1.89	0.85	−0.35	−3.67	−9.31	−9.02	11.39	10.55	−0.48	0.36	−0.04	0.02
2.39	0.66	−0.78	−2.69	−8.38	−3.18	12.04	9.95	−0.85	−1.41	−0.26	0.42
3.38	0.08	−1.29	−2.01	−3.88	1.56	7.22	7.14	−4.87	−2.01	0.09	1.06
4.38	2.65	0.83	−0.55	−1.03	0.52	−0.38	−2.98	−7.79	−4.11	1.68	3.69
5.38	4.99	1.86	0.14	−0.33	0.18	−3.14	−6.96	−9.04	−5.11	1.20	3.63
6.38	6.15	1.38	0.50	−1.11	−0.84	−4.05	−7.46	−8.98	−3.39	2.58	3.33
7.39	7.31	1.61	1.53	0.08	0.38	−3.52	−7.84	−9.38	−4.46	3.52	3.30
8.39	8.37	2.19	2.22	1.26	0.81	−2.66	−8.45	−10.91	−7.30	0.82	2.47
9.39	6.40	0.57	2.10	2.39	2.48	−1.73	−8.33	−10.13	−7.55	1.07	3.53

x-points and 150 y-points (for LSV). We recorded the errors (in basis points of spot, ie, as the absolute error in price over spot times $1E4$) between the surface values and the input values, the Dupire values and the input values, and the LSV values and the input values.

Note that ECP does not allow for bootstrap calibration unless the h-function parameters are fixed, and only σ values are calibrated. The full calibration can be done infrequently (eg, overnight), and fast bootstrap calibration can be applied instead during the day. Also, we recommend using the previous day's parameters as an efficient initial guess. The last point about calibration is that the choice of meta-parameters (such as the number of factors, the number of z-points and the various penalty coefficients) is very important, and occasionally an outside loop should be added to the calibration to determine the optimal values of these parameters for a given setup.

Our results can be found in the charts and tables on this page and the next.

Surface calibration errors are given in figure 3 and in table B. We also provide calibration error in volatility terms in figure 4. The resulting local volatility is given in figure 5. Dupire LV test errors are given in figure 6 and in table C. LSV test errors are given in figure 7 and in table D.

5 ECP local volatility surface

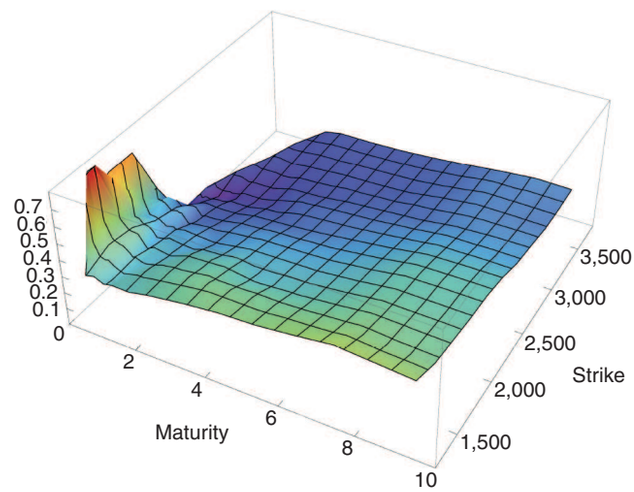

Conclusion

In this article, we have provided a simplified exposition of the CP surface, introduced a new arbitrage-free volatility surface with closed-form valuation and local volatility (ECP), and demonstrated the use of ECP in stochastic models (LV and LSV) with numerical examples. In our tests, we observed that the ECP surface fits well to options data with no-arbitrage conditions enforced, and that, when used in stochastic models, these compute the prices of the input options that are close to the input ones. ■

Alexandre Antonov is the chief analyst at Danske Bank in Copenhagen. Michael Spector is the vice-president, quantitative research at Numerix in New Jersey, and Michael Konikov is a senior vice-president and the head of quantitative development at Numerix in New York. They would like to thank Greg Whitten for his continuous support and Serguei Issakov for valuable discussions.

Email: antonov22@gmail.com, mkonikov1@gmail.com, spectormd@hotmail.com.

6 ECP Dupire repricing errors (spot basis points)

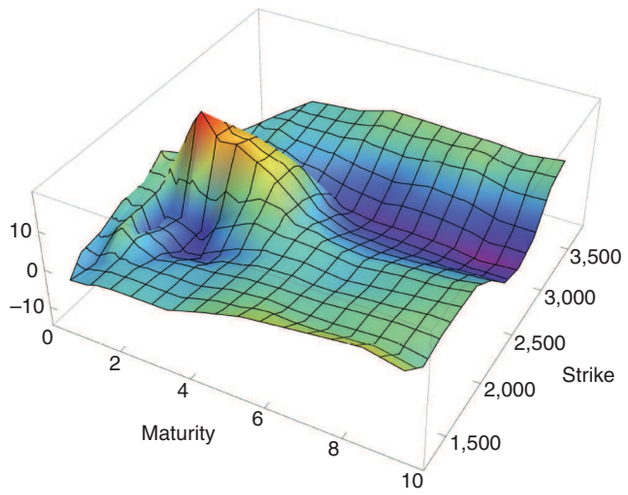

C. Dupire repricing errors (spot basis points) for ECP surface

	K										
T	1,238	1,486	1,733	1,981	2,229	2,476	2,724	2,972	3,219	3,467	3,715
0.05	—	—	—	—	−0.53	4.75	—	—	—	—	—
0.12	—	—	−1.55	1.34	1.43	3.47	—	—	—	—	—
0.22	—	−1.31	−2.40	1.32	1.54	3.07	−0.40	—	—	—	—
0.30	—	−2.09	−1.62	0.05	1.71	2.92	0.37	—	—	—	—
0.37	—	−2.35	−1.13	−0.08	1.84	3.19	2.14	—	—	—	—
0.62	−1.42	−2.96	0.88	0.81	1.28	3.18	5.80	−0.10	—	—	—
0.87	−1.26	−1.79	2.99	−6.44	−4.89	10.62	2.62	1.25	—	—	—
1.14	−1.04	−1.05	0.70	−3.08	−4.94	15.53	0.10	−0.79	0.43	—	—
1.39	−0.21	−0.58	−1.18	−3.67	−5.58	18.82	7.92	−2.54	−0.42	−0.29	—
1.89	0.23	−0.57	−3.18	−8.05	−7.67	12.41	10.95	−0.32	0.59	0.05	0.04
2.39	0.26	−0.68	−2.05	−7.30	−2.05	12.89	10.18	−0.66	−1.20	−0.10	0.49
3.38	0.27	−0.69	−0.98	−2.75	2.55	7.64	7.15	−5.01	−1.96	0.23	1.25
4.38	3.15	1.68	0.48	−0.08	1.16	−0.12	−3.15	−8.15	−4.21	1.74	3.85
5.38	5.64	2.73	1.05	0.44	0.66	−3.17	−7.11	−9.33	−5.38	1.17	3.65
6.38	6.83	2.18	1.26	−0.52	−0.47	−3.86	−7.51	−9.15	−3.66	2.31	3.23
7.39	7.99	2.36	2.22	0.62	0.74	−3.28	−7.86	−9.61	−4.72	3.26	3.08
8.39	9.09	2.96	2.90	1.80	1.17	−2.43	−8.38	−10.96	−7.38	0.72	2.29
9.39	7.08	1.28	2.74	2.92	2.85	−1.62	−8.28	−10.13	−7.54	1.09	3.53

7 ECP LSV repricing errors (spot basis points)

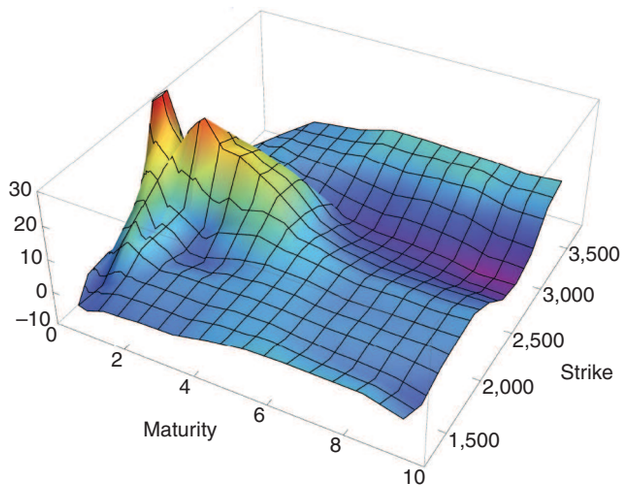

D. LSV repricing errors (spot basis points) for ECP surface. For the SV part, $\kappa = 0.3$, $\gamma = 0.2$ and $\rho = -0.5$

	K										
T	1,238	1,486	1,733	1,981	2,229	2,476	2,724	2,972	3,219	3,467	3,715
0.05	—	—	—	—	8.91	40.07	—	—	—	—	—
0.12	—	—	−1.55	−3.37	15.42	30.31	—	—	—	—	—
0.22	—	−1.31	−3.05	1.62	16.84	24.36	2.89	—	—	—	—
0.30	—	−2.09	0.27	6.51	16.71	22.12	4.38	—	—	—	—
0.37	—	−4.13	0.69	7.49	16.35	20.46	6.85	—	—	—	—
0.62	−2.65	−3.39	3.56	8.80	13.76	16.62	11.40	1.33	—	—	—
0.87	−3.50	−1.76	6.32	1.08	5.96	21.50	8.48	3.32	—	—	—
1.14	−2.49	−0.69	4.36	3.91	4.46	24.73	5.88	1.77	1.53	—	—
1.39	−1.55	−0.08	2.38	2.81	2.77	26.91	13.46	0.35	0.98	0.35	—
1.89	−1.30	0.15	0.10	−2.58	−0.90	19.06	16.12	2.89	2.42	1.04	0.54
2.39	−0.82	0.14	0.84	−2.70	3.47	18.40	14.91	2.64	0.89	1.16	1.22
3.38	−0.59	0.02	1.13	0.40	6.29	11.73	10.80	−1.90	0.39	1.93	2.42
4.38	1.68	1.72	1.72	2.05	3.91	2.79	−0.11	−5.33	−1.84	3.65	5.33
5.38	3.33	1.99	1.50	1.76	2.59	−0.68	−4.67	−6.95	−3.16	3.07	5.30
6.38	3.63	0.64	0.97	0.10	0.78	−2.28	−5.63	−7.19	−1.71	4.17	4.86
7.39	3.50	−0.25	0.97	0.37	1.19	−2.37	−6.52	−7.98	−3.01	4.93	4.67
8.39	3.35	−0.87	0.54	0.55	0.75	−2.27	−7.71	−9.93	−6.15	2.04	3.65
9.39	0.36	−3.53	−0.60	0.73	1.62	−1.97	−8.08	−9.57	−6.74	2.06	4.61

REFERENCES

Andreasen J and B Huge, 2011
Random grids
Risk July, page 62

Antonov A, M Konikov and M Spector, 2019
A new arbitrage-free parametric volatility surface
Preprint, SSRN, available at https://papers.ssrn.com/sol3/papers.cfm?abstract_id=3403708

Buehler H, 2018
Volatility and dividends II: consistent cash dividends
SSRN preprint, available at https://papers.ssrn.com/sol3/papers.cfm?abstract_id=2639318

Carr P and G Pelts, 2015
Duality, deltas, and derivatives pricing
Paper presented at a conference dedicated to Steve Shreve's 65th birthday, June

Carr P and G Pelts, 2017
Game of vols
SSRN preprint, available at https://papers.ssrn.com/sol3/papers.cfm?abstract_id=3422540

Cousot L, 2004
Necessary and sufficient conditions for no static arbitrage among European calls
Working Paper, October, Courant Institute, New York University

Dupire B, 1994
Pricing with a smile
Risk January, pages 18–20

Gatheral J, 2004
A parsimonious arbitrage-free implied volatility parameterization with application to the valuation of volatility derivatives
Paper presented at Global Derivatives & Risk Management Conference, Madrid

Gatheral J and A Jacquier, 2012
Arbitrage-free SVI volatility surface
Preprint, available at https://arxiv.org/abs/1204.0646v4

Gatheral J and A Jacquier, 2014
Arbitrage-free SVI volatility surface
Quantitative Finance 14, pages 59–71

Gyöngy I, 1986
Mimicking the one-dimensional marginal distributions of processes having an Ito differential
Probability Theory and Related Fields 71, pages 501–516

Lipton A, 2002
The vol smile problem
Risk February, pages 61–65

Lucic V, 2020
Lecture notes on `Volatility modelling'
Imperial College London, available at https://jackantoinejacquier.wixsite.com/jacquier/volatility-modelling

Madan D, M Qian and Y Ren, 2007
Calibrating and pricing with embedded local volatility models
Risk September, pages 138–143